Benzodiazepinedione inhibitors of the Hdm2:p53 complex suppress human tumor cell proliferation *in vitro* and sensitize tumors to doxorubicin *in vivo*

Holly K. Koblish, Shuyuan Zhao, Carol F. Franks, Robert R. Donatelli, Rose M. Tominovich, Louis V. LaFrance, Kristi A. Leonard, Joan M. Gushue, Daniel J. Parks, Raul R. Calvo, Karen L. Milkiewicz, Juan José Marugán, Pierre Raboisson, Maxwell D. Cummings, Bruce L. Grasberger, Dana L. Johnson, Tianbao Lu, Christopher J. Molloy, and Anna C. Maroney

Johnson & Johnson Pharmaceutical Research and Development, L.L.C., Spring House, Pennsylvania

Abstract

The activity and stability of the p53 tumor suppressor are regulated by the human homologue of the mouse double minute 2 (Hdm2) oncoprotein. It has been hypothesized that small molecules disrupting the Hdm2:p53 complex would allow for the activation of p53 and result in growth suppression. We have identified small-molecule inhibitors of the Hdm2:p53 interaction using our proprietary ThermoFluor microcalorimetry technology. Medicinal chemistry and structure-based drug design led to the development of an optimized series of benzodiazepinediones, including TDP521252 and TDP665759. Activities were dependent on the expression of wild-type (wt) p53 and Hdm2 as determined by lack of potency in mutant or null p53-expressing cell lines or cells engineered to no longer express Hdm2 and wt p53. TDP521252 and TDP665759 inhibited the proliferation of wt p53-expressing cell lines with average IC_{50}s of 14 and 0.7 μmol/L, respectively. These results correlated with the direct cellular dissociation of Hdm2 from wt p53 observed within 15 minutes in JAR choriocarcinoma cells. Additional activities of these inhibitors *in vitro* include stabilization of p53 protein levels, up-regulation of p53 target genes in a DNA damage–independent manner, and induction of apoptosis in HepG2 cells. Administration of TDP665759 to mice led to an increase in $p21^{waf1/cip1}$ levels in liver samples. Finally, TDP665759 synergizes with doxorubicin both in culture and in an A375 xenograft model to decrease tumor growth. Taken together, these data support the potential utility of small-molecule inhibitors of the Hdm2:p53 interaction for the treatment of wt p53-expressing tumors. [Mol Cancer Ther 2006;5(1):160–9]

Introduction

The p53 tumor suppressor protein is a DNA damage–inducible transcription factor that contributes to both cell cycle arrest and apoptosis. The tumor suppressor activity associated with p53 is most prominently shown by the high rate of spontaneous tumor development in p53 knockout mice (1). Furthermore, the activity of wild-type (wt) p53 is central to the positive response of tumors to various therapeutic regimens. Tumors that express null or mutant forms of p53 are associated with poorer prognosis and chemoresistance or radioresistance (2–8). Approximately half of all human cancer types have inactivated or mutant p53, supporting the concept that loss of p53 contributes to tumorigenesis (9). Therefore, it has been proposed that up-regulation of wt p53 activity in tumors could be of therapeutic benefit (10–12).

Hdm2, the major intracellular negative regulator of p53, is also a transcriptional target of p53, and as such, Hdm2 acts in a negative feedback loop to tightly regulate wt p53 activity (13). Inactivation of the *Hdm2* gene locus causes embryonic lethality in mice; however, this phenotype can be rescued when it is crossed with p53 null mice. Thus, the major function of Hdm2 is to suppress p53 function *in vivo* (14, 15). Hdm2 controls intracellular regulation of p53 levels in two ways. First, through its direct binding to p53 and subsequent occlusion of the site necessary for binding to the transcriptional machinery, Hdm2 can inhibit p53 growth-suppressive functions (16). Second, Hdm2 has ubiquitin ligase activity, which targets p53 for destruction via the cellular proteasome pathway (17). As in tumors expressing mutant or null p53, overexpression of Hdm2 by tumors is also associated with poor prognosis (18–20).

Reports of enhanced tumor cell death following disruption of the Hdm2:p53 interaction by Hdm2 antisense or p53 peptidomimetics indicate that inhibition of the Hdm2:p53 interaction will activate p53 and in turn trigger cell cycle

Received 6/17/05; revised 9/21/05; accepted 11/2/05.

The costs of publication of this article were defrayed in part by the payment of page charges. This article must therefore be hereby marked advertisement in accordance with 18 U.S.C. Section 1734 solely to indicate this fact.

Note: L.V. LaFrance is currently at GlaxoSmithKline, Inc., 1250 South Collegeville Road, Collegeville, PA 19426. J.M. Gushue is currently at ICON Clinical Research, 212 Church Road, North Wales, PA 19454. K.L. Milkiewicz is currently at Cephalon, Inc., 145 Brandywine Parkway, West Chester, PA 19380. P. Raboisson is currently at Tibotec, Gen De Wittelaan L 11B 3, 2800 Mechelen, Belgium.

Requests for reprints: Holly K. Koblish, Johnson & Johnson Pharmaceutical Research and Development, L.L.C., Welsh and McKean Roads, Spring House, PA 19477. Phone: 215-628-5449; Fax: 215-628-5047. E-mail: hkoblis1@prdus.jnj.com

doi:10.1158/1535-7163.MCT-05-0199

arrest or apoptosis (21–24). Antisense to Hdm2 in combination with chemotherapeutic agents show that inhibiting the interaction between p53 and Hdm2 should be additive or synergistic with standard chemotherapeutic agents in the treatment of certain neoplasms (25). Despite limited success, gene therapy approaches to induce wt p53 expression have been approved in China for the treatment of head and neck squamous cell carcinoma (26, 27). Compared with these approaches, a small-molecule inhibitor of the Hdm2:p53 interaction would be advantageous due to uniform exposure to the tumor cells and facile administration. We have reported recently our effort to discover small-molecule inhibitors of the Hdm2:p53 interaction using ThermoFluor microcalorimetry and to use crystallography to assist in structure-based drug design (28). Herein, we describe the molecular and cellular events triggered by these small-molecule inhibitors of the Hdm2:p53 interaction in cells and further show synergistic effects *in vivo* in combination with the DNA-damaging agent doxorubicin.

Materials and Methods

Cell Lines

JAR choriocarcinoma cells (HTB-144) and HepG2 hepatocellular carcinoma cells (HTB-8065), both from American Type Culture Collection (Manassas, VA), were maintained in RPMI and EMEM supplemented with 10% fetal bovine serum, respectively. The mdm2/p53 double-null and mdmX/p53 double-null cell lines were the generous gift of Dr. Guillermina Lozano (University of Texas M.D. Anderson Cancer Center, Houston, TX) and were maintained as described (29).

Proliferation Assay

Cells were seeded at 1,000 per well in 96-well plates. After allowing for adherence overnight, cells were treated with various concentrations of compounds for 3 days. Cells were labeled with bromodeoxyuridine for the last 6 hours of compound exposure and then fixed and assayed by ELISA according to the manufacturer's instructions (Bromodeoxyuridine Cell Proliferation Assay, Exalpha, Watertown, MA). IC_{50}s were determined using Prism software (GraphPad Software, San Diego, CA).

Coimmunoprecipitation and Immunoblot Assay

JAR choriocarcinoma cells were treated with increasing doses of compounds for 90 minutes followed by lysis in Triton X-100 buffer [1% Triton X-100, 10 mmol/L Tris (pH 7.2), 5 mmol/L EDTA, 50 mmol/L NaCl, Complete Mini protease inhibitor cocktail tablets (Roche Applied Science, Indianapolis, IN), and phosphatase inhibitor cocktails 1 and 2 (Sigma-Aldrich, St. Louis, MO)]. Lysates were normalized to protein and immunoprecipitated with an anti-p53 antibody (FL-393, Santa Cruz Biotechnology, Santa Cruz, CA). Immunoprecipitates were washed twice in lysis buffer followed by resuspension in electrophoresis sample buffer. Samples were separated on a 4% to 12% Bis-Tris polyacrylamide gels with 1× MOPS running buffer (Invitrogen, Carlsbad, CA), transferred to nitrocellulose membranes, blocked with 5% nonfat dry milk in TBS/0.1% Tween 20, and probed in the same buffer with anti-p53 (DO-1, Oncogene Research Products, Boston, MA), anti-Hdm2 (SMP-14, Santa Cruz Biotechnology), or anti-actin (I-19, Santa Cruz Biotechnology). Relative ratios were determined after scanning images generated using Typhoon scanner (Molecular Dynamics, Sunnyvale, CA). Ratios were determined by ImageQuant analysis and were expressed as percent bound to p53 relative to the vehicle control.

Detection of Proteins from Total Lysate

HepG2 cells were treated for 24 hours with TDP521252 and lysed in Triton X-100 buffer, and protein extract (30 μg) was denatured and separated by SDS-PAGE. Gels were electroblotted as described above. Antibodies for immunoblotting included anti-Hdm2 2A10 hybridoma supernatant (gift from Dr. Mary Ellen Perry, NCI, Bethesda, MD), anti-p53 (Ab-6, Oncogene Research Products), anti-$p21^{waf1/cip1}$ (F-5, Santa Cruz Biotechnology), anti-phospho-p53 (Cell Signaling Technology, Beverly, MA), and anti–p53 up-regulated modulator of apoptosis (PUMA; Ab-1, Oncogene Research Products). SuperSignal West Pico Chemiluminescent Substrate (Pierce, Rockford, IL) was used to detect the proteins of interest, and blots were quantitated using either Scion Image Analysis (Scion Corp., Frederick, MD) or Typhoon scanner.

Quantitative Real-time PCR Analysis of p53 Target Genes

Samples for quantitative real-time PCR analysis were obtained from either HepG2 cells or mouse tissue. HepG2 cells were seeded at 6×10^5 per well in a six-well plate overnight. The following morning, cells were treated with compounds or DMSO over an 8-hour time course. Total RNA was isolated using the RNeasy kit (Qiagen, Valencia, CA) according to the manufacturer's protocol. Female BALB/c *nu/nu* mice were given TDP665759 (25 or 50 mg/kg) twice daily for a total of seven doses i.p. (12 hours apart) or doxorubicin (10 mg/kg) once i.v. 24 hours before tissue collection. Six hours after the final dose of TDP665759, the mice were sacrificed and livers were harvested and flash frozen on dry ice in tubes containing RNeasy and total RNA was isolated as described above.

Real-time PCR using RNA as the initial template was done on these samples using the Taqman One-Step RT-PCR Master Mix Reagent (Applied Biosystems, Foster City, CA). Fluorescently tagged primer/probe mixtures were purchased from Applied Biosystems for human glyceraldehyde-3-phosphate dehydrogenase, Hdm2, PUMA, p53, $p21^{waf1/cip1}$, and p53-inducible gene-3 and were designed to span an intron/exon boundary to discount genomic DNA contamination. All samples were normalized to glyceraldehyde-3-phosphate dehydrogenase and quantified using the standard curve method. Reactions were carried out in an ABI Prism 7000 (Applied Biosystems).

H2AX Phosphorylation Assay

JAR choriocarcinoma, HepG2 hepatocellular carcinoma, and A375 melanoma cells were seeded at 10,000 per well in 96-well plates and allowed to adhere overnight. Cells were

then treated with 40 μmol/L TDP521252 or TDP536356, 5 μmol/L doxorubicin, or 50 μmol/L topotecan for 2 hours, processed, and analyzed for phosphorylated H2AX using the H2AX Phosphorylation Chemiluminescent Assay (Upstate, Charlottesville, VA).

Caspase Assay

HepG2 hepatocellular carcinoma cells were treated with 40 μmol/L TDP521252, TDP536356, or DMSO for 0, 8, 16, 24, or 48 hours. Cells were lysed and exposed to substrates for caspase-3 and caspase-7 (ApoOne, Promega, Madison WI) and specific processing was measured over 2 hours. Rates of caspase activity were then calculated using the differential results at 20 and 40 minutes after substrate addition.

Hoechst Staining

For assessing apoptotic nuclei, HepG2 cells were plated onto four-chamber SonicSeal slides (Nunc, Naperville, IL). After exposure to compound, cells were fixed with 3.7% formaldehyde for 15 minutes, rinsed in PBS, and subsequently stained with 2.5 μg/mL Hoechst dye for 15 minutes. After staining, cells were rinsed again and mounted using Prolong Antifade (Molecular Probes, Eugene, OR) and then examined and photographed with an Olympus IX81 microscope (Melville, NY).

Cell Culture Drug Combination Studies

A375 melanoma cells (ATCC CRL-1619) were seeded at 2,000 per well in 96-well white-walled plates and allowed to adhere overnight. Chemotherapeutic agents and TDP665759 were added at the same time in a fixed ratio format. Cells were exposed to compound for 48 hours and viability of cells was determined using Cell-Titer-Glo (Promega). Calculations of combination effects were done according to the method of Chou and Talalay (30) using CalcuSyn software (Biosoft, Cambridge, United Kingdom). Combination indices of <0.9 are synergistic, between 0.9 and 1.1 are additive, and >1.1 are antagonistic. For the determination of p53 levels in combination-treated cells, A375 melanoma cells were seeded at 5,000 per well in 96-well plates and allowed to adhere overnight. After cells were treated with the IC_{50} of each of doxorubicin (0.2 μmol/L) and TDP665759 (2 μmol/L) and the combination for 24 hours, cells were lysed and p53 levels were determined using the PathScan Total p53 Sandwich ELISA (Cell Signaling Technology).

A375 Xenograft Study

An A375 melanoma xenograft study was done at Piedmont Research Center, Inc. (Morrisville, NC) in female nude mice (Harlan, Indianapolis, IN). After tumors reached 80 to 120 mg in size, mice were randomized into treatment groups and treatment with vehicle (20.25% hydroxypropyl-β-cyclodextran, b.i.d. × 10), 100 mg/kg TDP665759 (p.o., b.i.d. × 10), 1.5 or 3 mg/kg doxorubicin (i.v., q.d. × 5), or a combination of 100 mg/kg TDP665759 (p.o., b.i.d. × 10) and 1.5 mg/kg doxorubicin (i.v., q.d. × 5) was initiated. Mice were monitored daily for general health and tumor size was measured every third or fourth day. Mice were euthanized when tumor volume exceeded 2 g.

Results

Inhibitors of the Hdm2:p53 Interaction Suppress Tumor Cell Proliferation

We have reported previously the identification of novel small-molecule inhibitors of the Hdm2:p53 interaction using ThermoFluor microcalorimetry, which detects a shift in the intrinsic melting temperature of protein bound to compound (28, 31, 32). A benzodiazepinedione series identified from this screening effort was further optimized for *in vitro* potency in a fluorescence polarization assay that detects the displacement of fluorescently labeled p53 peptide from an amino-terminal fragment of the Hdm2 protein (28). The *in vitro* potencies of specific active enantiomers from the benzodiazepinedione series exhibited IC_{50}s from 0.3 to 0.7 μmol/L that were substantially different from those of the related inactive enantiomers (Fig. 1). One example, TDP222669, is a relatively potent Hdm2 inhibitor *in vitro* with an IC_{50} of 0.57 μmol/L. The cellular potency of this compound was poor, however, most likely due to low cell permeability. Efforts to advance this chemical series were focused on increasing cellular permeability. In this regard, replacement of the acid moiety of TDP222669 with a methyl group and introduction of a valeryl (TDP521252) or a 3-(4-methylpiperazin-1-yl)propyl (TDP665759) solubilizing moiety at position 1 of the 1,4-benzodiazepine-2,5-dione created compounds with roughly equivalent *in vitro* potencies relative to TDP222669 but ~3- to 66-fold improved cellular activity (Table 1).

The antiproliferative activities of TDP222669 and TDP-521252 were measured across a panel of human tumor cell lines. TDP521252 was 3-fold more potent, on average, than TDP222669 against cells expressing wt p53 (Table 1). Further, TDP665759 was ~22-fold more potent then TDP521252, with an average IC_{50} in cells expressing wt

Structure	Compound	FP IC_{50} (μmol/L)
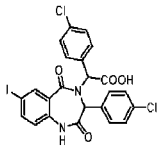	TDP222669 (S,S) (R,R) racemate	0.567 ± 0.055
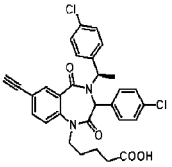	TDP521252 (3S) active enantiomer	0.708 ± 0.002
	TDP536356 (3R) inactive enantiomer	28.5 ± 2.55
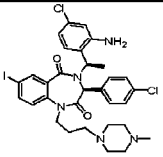	TDP665759	0.704 ± 0.06

Figure 1. Benzodiazepinedione inhibitors of the Hdm2:p53 interaction.

Table 1. Inhibitors of the Hdm2:p53 interaction selectively block proliferation of wt p53 tumor cell lines

	IC_{50} (μmol/L), mean ± SE	
	TDP222669	TDP521252
wt p53		
MCF7	33.3 ± 17.5	10.0 ± 2.0
A375	46.5 ± 12.0	12.0 ± 3.5
HepG2	45.5 ± 10.8	11.0 ± 3.7
A498	47.7 ± 10.8	13.0 ± 1.9
HCT116	58.0 ± 3.0	14.8 ± 1.5
LNCaP	ND	4.7 ± 1.5
ZR75-1	ND	19.0 ± 6.0
JAR*	33.8 ± 3.6	19.0 ± 3.7
SJSA*	ND	13.8 ± 2.6
JEG3*	ND	46.5 ± 6.1
Mutant/null p53		
MDA-MB-231 (mutant)	132.1 ± 16.7	69.7 ±16.2
Panc1 (mutant)	>200	>200
SK-BR-3 (mutant)	ND	30.5 ± 3.8
DU145 (mutant)	ND	66.5 ± 22.4
MiaPaCa (mutant)	>200	141.7 ± 7.6
A431 (mutant)	>200	123.8 ± 37.9
PC3 (null)	ND	41.5 ± 9.3
SK-OV-3 (null)	ND	69.8 ± 6.2
H1299 (null)	183.3 ± 28.9	101.3 ± 62.4

NOTE: Cells were seeded at 1,000 per well in 96-well plates and allowed to adhere overnight. Cells were then exposed to compound dilutions (1.56–100 μmol/L for wt p53 and 3.125–200 μmol/L for mutant and null p53 cell lines) for 72 hours. Six hours before fixation and processing according to the manufacturer's specifications, cells were labeled with bromodeoxyuridine. Prism software was used to calculate the IC_{50}s (mean ± SE) of three separate experiments, each condition done in triplicate.
*Cells overexpressing Hdm2.

p53 of 0.7 μmol/L (data not shown). As would be predicted for an indirect p53 agonist, these compounds were less effective at controlling the growth of tumor cells expressing mutant or null p53. The enhanced cellular potency observed against cells expressing wt p53 correlated with decreased activity in mutant or null p53 cell lines. The window of growth inhibitory activity between wt and mutant/null p53 cell lines for TDP222669 was ~4-fold and similar to that obtained with TDP521252 (Table 1). The sensitivity of wt p53-expressing cells increased to >10-fold, on average, when cells were treated with TDP665759, with an IC_{50} of 0.5 μmol/L in MCF7 (wt p53) cells versus >5 μmol/L in MDA MB 231 (mutant p53) cells (data not shown).

Benzodiazepinediones Rapidly Cause the Dissociation of Cellular Hdm2 from p53

It was critical to our understanding of the functional outcomes of treating cells with the benzodiazepinediones to study the direct effect of these compounds on the Hdm2:p53 complex in cells. For these studies, JAR choriocarcinoma cells were used because they have higher and thus more readily detectable basal levels of Hdm2 and p53 (33). JAR cells were treated for 90 minutes with TDP521252 or the inactive enantiomer TDP536356, lysed, normalized for protein, and subjected to immunoprecipitation with an anti-p53 antibody. As shown in Fig. 2A, there is a striking dose-dependent decrease in the amount of Hdm2 associated with p53 that is observed in the presence of inhibitors. At a concentration of 40 μmol/L, 2-fold greater than the IC_{50} for inhibition of cell proliferation, TDP521252 caused >90% dissociation of Hdm2 from p53. Similar results have been observed as early as 15 minutes after treating cells with compounds (data not shown). In contrast, the inactive enantiomer, TDP536356, failed to cause significant dissociation of Hdm2 from p53 (Fig. 2A). These results are more striking when the increase in total Hdm2 and p53 levels relative to steady total actin levels are compared with the amount of Hdm2 remaining associated with p53 in the presence of the active enantiomer (Fig. 2A). As expected, these data show that initial release of p53 from Hdm2 results in an increase in Hdm2 levels and that these higher levels of Hdm2 do not interact with p53 in the presence of active enantiomer in the cell.

It is well understood that p53 can be stabilized after cells are exposed to DNA-damaging agents or environmental stress. Multiple kinases have been shown to phosphorylate specific sites on p53 leading to release of p53 from Hdm2 and activating downstream target gene expression (34, 35). To confirm that DNA damage was not the mechanism by which the benzodiazepinediones were causing p53 release from Hdm2, we examined two DNA damage–inducible phosphorylation events. First, we analyzed the Ser^{15} residue of p53 in HepG2 cells exposed to TDP521252 or the inactive enantiomer TDP536356. As would be predicted, only TDP521252, but not TDP536356, increased the level of total p53 (Fig. 2B). As a positive control, treatment of HepG2 cells with the topoisomerase II inhibitor doxorubicin led to an increase in phosphorylation at Ser^{15} concomitant with the increase in total p53 in agreement with previous reports (36). Neither TDP521252 nor TDP536356 caused the phosphorylation of p53 at Ser^{15} (Fig. 2B). The lack of phosphorylation at Ser^{15} as well as other phosphorylation sites on p53 has been reproduced in A375 melanoma and HCT116 colon carcinoma cells (data not shown). We also examined the phosphorylation of H2AX, another indicator of DNA damage, in response to TDP521252, TDP536356, and the known DNA-damaging agents topotecan and doxorubicin in JAR choriocarcinoma, HepG2 hepatocellular carcinoma, and A375 melanoma cells (Fig. 2C). Although there was substantial phosphorylation of H2AX induced by both of the known DNA damage inducers in these cell lines after 2 hours, there was no phosphorylation induced by the Hdm2 inhibitors at twice the IC_{50} concentrations in any of the cell lines tested. The lower phosphorylation of H2AX in HepG2 when compared with the other cell lines is consistent with a previous report that the HepG2 cell line is not particularly sensitive to DNA-damaging agents (37). These data, taken together with our crystal structure (28), window of activity between cell lines expressing wt and mutant or null p53, and lack of DNA damage pathway activation, support the concept that disruption of the Hdm2:p53 interaction is the principal mechanism of action of the Hdm2-directed benzodiazepinediones.

Biochemical Outcome of Stabilizing p53 in HepG2 Cells Treated with TDP521252

Stabilization of p53 results in the up-regulation of a multitude of genes involved in diverse activities, including regulation of cell cycle and apoptosis (38, 39). Therefore, it was of interest to show that inhibitors of the Hdm2:p53 complex modulated p53-regulated genes and their translated proteins. In particular, p53-inducible gene-3, PUMA, Hdm2, and $p21^{waf1/cip1}$ were examined due to their involvement in the cell cycle and apoptosis (39, 40). HepG2 hepatocellular carcinoma cells were treated with 20 μmol/L TDP521252 or the inactive enantiomer TDP536356 for various times over an 8-hour period (Fig. 3A). Early mRNA induction was observed for $p21^{waf1/cip1}$ and Hdm2 peaking after 4-hours exposure to TDP521252, with increases in PUMAα and p53-inducible gene-3 following at later time points. The time course of early and late induction of these genes is consistent with previously reported results of promoter occupancy (41). In contrast, no induction of $p21^{waf1/cip1}$ (or the other p53-regulated genes; data not shown) was observed following treatment of the cells with either DMSO or the inactive enantiomer, TDP536356 (Fig. 3A). A similar profile was observed in JAR choriocarcinoma cells (data not shown).

To show that the induction of p53-regulated mRNA by TDP521252 resulted in increased protein expression, HepG2 cells were treated with increasing doses of TDP521252 for 24 hours followed by immunoblot analysis of lysates from treated samples. We observed dose-dependent increases in p53-regulated protein expression in all instances. At the highest dose of TDP521252 tested (40 μmol/L), the greatest induction of protein relative to untreated controls was observed with PUMAα (84 times) followed by $p21^{waf1/cip1}$ (67 times) and Hdm2 (45 times; Fig. 3B). Furthermore, the level of p53 protein was ~3-fold higher after 24 hours in the presence of 40 μmol/L TDP521252 (Fig. 3B). The increase in p53 protein was not due to changes in mRNA expression (Fig. 3A) but rather was most likely due to inhibition of the ubiquitination of p53 induced by Hdm2 E3 ligase activity when p53 is bound to Hdm2 (17). Overall, these data clearly show that stabilization of p53 by TDP521252 leads to the increased expression of p53-regulated genes.

TDP521252 Induces Apoptosis in HepG2 Cells

Activation of p53 in tumor cell lines can lead to either a cytostatic or an apoptotic event depending on the cellular environment (39). In anticipating the effect of an Hdm2:p53 inhibitor on tumor growth in xenografts, it was essential to determine whether such an inhibitor would act as a cytostatic agent and prevent further tumor growth or induce programmed cell death and potentially lead to tumor regression. To address this question, two parameters of programmed cell death, caspase activity and chromatin condensation, were examined in HepG2 cells. The rate of caspase-3 and caspase-7 activation in cells treated with the active enantiomer TDP521252 is substantially increased compared with that observed for cells treated with either DMSO or the inactive enantiomer TDP536356 (Fig. 4A). The induction of caspases was observed as early as 16 hours after addition of TDP521252 and increased ~4.5-fold over the following 32 hours. In additional studies, asynchronous HepG2 cells were exposed to both the active and the inactive enantiomers of TDP521252 over a 3-day period after which time cells were harvested, fixed, and stained with Hoechst dye to detect chromatin. Exposure to the active enantiomer caused an accumulation of condensed chromatin as seen by punctate staining of the nuclei (Fig. 4B). Taken together, these data indicate that inhibition of the Hdm2 interaction with p53 in HepG2 cells leads to activation of an apoptotic response in HepG2 cells.

Induction of the $p21^{waf1/cip1}$ Biomarker *In vivo* by an Inhibitor of the Hdm2:p53 Interaction

Over the course of optimizing the benzodiazepinedione series, we identified compounds with comparable *in vitro*

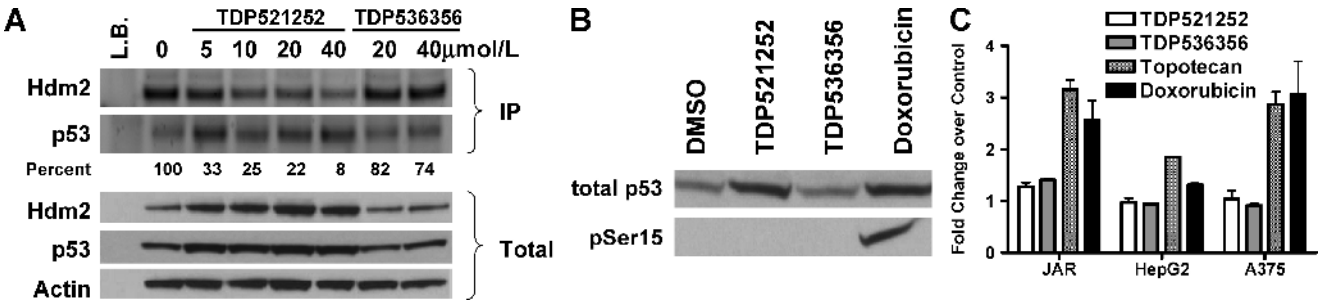

Figure 2. Benzodiazepinedione inhibitors cause the dissociation of Hdm2 from p53 in cells without inducing DNA damage. **A,** JAR choriocarcinoma cells were treated with TDP521252 (active enantiomer) and TDP536356 (inactive enantiomer) for 90 min followed by lysis, normalization to protein, and immunoprecipitation with anti-p53 antibody. Immunoblots of total lysates probed with anti-actin (I-19) are shown as an indicator of normalized protein and probed with anti-Hdm2 and anti-p53 as a measure of input protein. The immunoprecipitates were resolved by electrophoresis, transferred to nitrocellulose membrane, and immunoblotted with either anti-Hdm2 or anti-p53 antibodies. Percent indicated is the ratio of Hdm2:p53 as normalized to vehicle control. **B,** HepG2 hepatocellular carcinoma cells were treated with 20 μmol/L TDP52152 or TDP536356 or 1 μmol/L doxorubicin for 24 h. Cells were then lysed and normalized to protein. Total lysate was resolved by electrophoresis, transferred to a nitrocellulose membrane, and immunoblotted with antibodies recognizing either total or phosphorylated p53. **C,** JAR choriocarcinoma, HepG2 hepatocellular carcinoma, and A375 melanoma cells were seeded and allowed to adhere overnight before treatment with 40 μmol/L TDP521252 or TDP536356 or 5 μmol/L doxorubicin or 50 μmol/L topotecan for 2 h. Cells were processed and lysates analyzed for H2AX phosphorylation according to the manufacturer's recommendations.

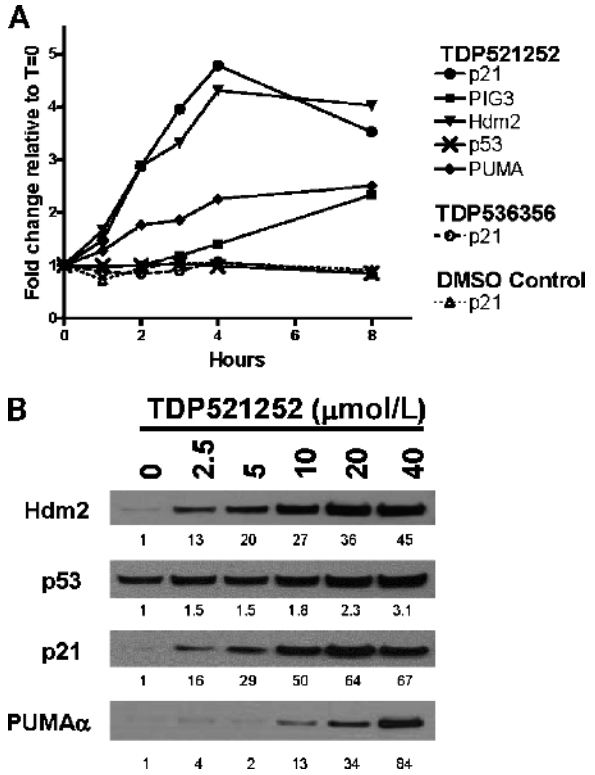

Figure 3. TDP521252 regulates the p53 pathway. **A,** HepG2 hepatocellular carcinoma cells were subjected to TDP52152 or TDP536356 for 1, 2, 4, or 8 h and total cellular RNA was harvested. Quantitative real-time PCR was done to determine the up-regulation of the p53 target genes. Results were normalized to glyceraldehyde-3-phosphate dehydrogenase and are expressed as fold increase relative to time 0. Representative of one of two separate experiments. **B,** HepG2 cells were treated with increasing doses of TDP521252 for 24 h. Total cellular protein was harvested and lysates were subjected to immunoblot analysis for Hdm2, p53, $p21^{waf1/cip1}$, and PUMAα. Data are fold increase over vehicle control. Representative of one of two separate experiments.

antiproliferative potencies as TDP521252 but with enhanced cellular permeability. In this regard, the compound TDP665759 inhibited wt p53-expressing MCF7 breast carcinoma cells with an average IC_{50} of 0.73 ± 0.21 μmol/L (three separate experiments), a 14-fold improvement over TDP521252. Similar to TDP521252, TDP665759 did not significantly inhibit the proliferation of mutant p53 MDA-MB-231 cells, with an IC_{50} of >5 μmol/L. To begin to address whether these inhibitors could induce p53 activation *in vivo*, we established a pharmacodynamic assay to measure induction of $p21^{waf1/cip1}$ mRNA from various tissues after treating mice with benzodiazepinediones. Doxorubicin has been shown previously to activate p53 and was therefore used as a positive control (42). The benzodiazepinediones and doxorubicin induced $p21^{waf1/cip1}$ message to the greatest extent in liver (Fig. 5A), with lesser but measurable induction in thymus and spleen, respectively (data not shown). The highest sensitivity of the liver to these agents is consistent with $p21^{waf1/cip1}$ induced by γ-irradiation in wt p53 transgenic mice (43). Mice were given TDP665759 i.p. at 25 and 50 mg/kg twice for a total of seven doses or doxorubicin once i.v. 24 hours before sacrifice. In these experiments, the compound was well tolerated at the 25 mg/kg dose; however, the 50 mg/kg group experienced some body weight loss (16%) by the end of the 4-day study. Liver tissues were retrieved 6 hours after the final compound administration and analyzed by real-time PCR to determine the change in $p21^{waf1/cip1}$ mRNA. Administration of 25 mg/kg TDP665759 produced a 30-fold induction of $p21^{waf1/cip1}$ relative to vehicle control and was similar to induction by doxorubicin treatment (Fig. 5A). At the 50 mg/kg dose, induction was >150-fold relative to vehicle control. The exponential-like effect of $p21^{waf1/cip1}$ mRNA induction suggests the possibility of positive feedback loops and has been observed with other compounds in this chemical series (data not shown). These results show *in vivo* target-based activity of the benzodiazepinediones.

TDP665759 Potentiates Doxorubicin in Cell Culture and in A375 Xenografts

It has been hypothesized that activating p53 in combination with chemotherapy or radiotherapy would result in enhanced antitumor activity (44). This has been shown preclinically with antisense to Hdm2 in a variety of prostate cancer, breast cancer, and glioma models (45–48) and recently in a phase II study using a combination of a replication-deficient adenovirus expressing wt p53 and doxorubicin in patients with locally advanced breast cancer (49). To test this hypothesis with small-molecule inhibitors of the Hdm2:p53 interaction, A375 melanoma cells (50) were treated with TDP665759 in combination with a variety of chemotherapeutic agents. Using a fixed ratio combination approach (30), TDP665759 synergized with doxorubicin, 5-fluorouracil, and irinotecan (Fig. 5B). In contrast, combination of TDP665759 and cisplatin resulted in an antagonistic effect.

Hypothesizing that the combination of Hdm2 inhibition and treatment with a DNA-damaging agent would enhance p53 stabilization, we sought to determine the molecular basis for this synergy by analyzing total p53 levels in A375 melanoma cells treated with TDP665759, doxorubicin, and the combination of the two agents for 24 hours. We found that treatment of A375 cells with TDP665759 or doxorubicin alone resulted in a 4- and 6-fold increase in p53 levels over DMSO-treated cells, respectively (Fig. 5C). When these agents were added together, p53 levels rose 18-fold over control. These data support that the molecular mechanism of the synergy is to enhance p53 stabilization.

Based on these results, doxorubicin was selected for testing in combination with TDP665759 in an A375 xenograft model. The dose of TDP665759 was chosen based on the maximum tolerated dose in combination with doxorubicin. The dosing concentration of TDP665759 alone was not expected to achieve significant efficacy based on pharmacokinetic profiles of the compound. As can be seen in Fig. 5D, TDP665759 (100 mg/kg) elicits only a modest effect on A375 tumor growth but trends toward a significant difference from that seen in vehicle-treated animals (P = 0.0513 at day 15, Mann-Whitney test). The low dose of doxorubicin

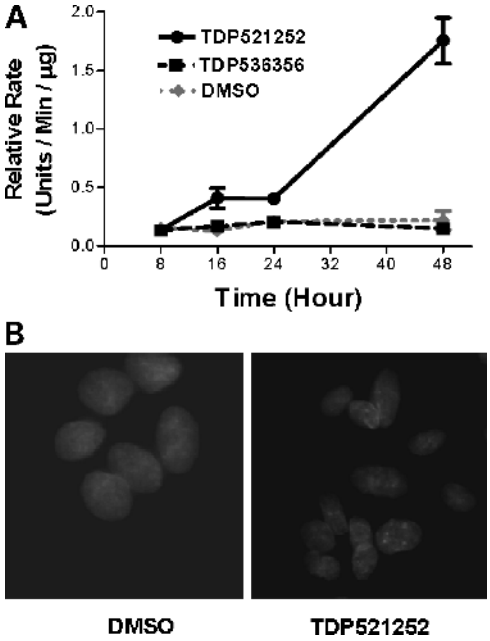

Figure 4. TDP521252 induces apoptosis in HepG2 cells. **A,** TDP521252 induces caspase-3 and caspase-7 activity. HepG2 cells were treated with TDP521252, TDP536356, or vehicle control for 8 to 48 h as indicated. At the end of the time points, cells were lysed, caspase substrate was added, and activity was measured every 20 min for 2 h. Specific activity is reported as the rate of activity per minute per microgram of total protein for the period between 20 and 40 min after substrate addition. **B,** TDP521252 induces chromatin condensation. HepG2 cells were exposed to TDP521252 for 72 h, fixed with formaldehyde, and stained with Hoechst dye. Cells were visualized and photos were taken using Olympus IX81.

(1.5 mg/kg = 0.5 maximum tolerated dose) did not result in any significant difference in tumor growth from the vehicle-treated animals ($P = 0.4079$, Mann-Whitney test). However, combining TDP665759 and 1.5 mg/kg doxorubicin resulted in tumor growth inhibition similar to that resulting from treatment with 3 mg/kg doxorubicin (tumor growth inhibition of 79% versus 74% on day 15, respectively). These two treatment paradigms were also similar in the delay to reach the study end point of 2,000 mg (28.0 days for 3 mg/kg doxorubicin and 26.9 days for the combination versus 16.1 days for vehicle-treated mice). Interestingly, the body weight loss was greater in the mice that received the maximum tolerated dose of doxorubicin alone (20% on day 15) than in the mice that received the combination (8.4% on day 15), indicating that reduction in dose of chemotherapeutic agents can reduce toxicity. These data support the prevailing hypothesis that a DNA-damaging chemotherapeutic agent would synergize with an agent that prolongs induction of p53, and importantly, these data are the first to show this synergy when p53 is induced using a small-molecule inhibitor of the p53:hdm2 interaction.

Discussion

p53 has been called the ''cellular gatekeeper'' presiding over key processes involved in determining whether a cell lives or dies. Its involvement in cellular growth regulation is evidenced by the robust and spontaneous tumor development observed in p53 knockout mice (51). Approximately one-half of human tumors have lost the ability to activate wt p53, further suggesting a key role for this tumor suppressor (52, 53). Based on these observations, approaches to activating wt p53 have been a target of intense research for the potential to treat a variety of human cancers. The most advanced clinical attempts to express wt p53 in solid tumors involve gene therapy with adenoviral vectors or the use of recombinant viruses. To date, the clinical results have been disappointing possibly due to difficulty in delivery, the maintenance of long-term expression, or the formation of nonfunctional tetramers containing both wt and mutant p53 (27, 54). Hdm2 antisense approaches are in the discovery stage (21, 22, 33). Small-molecule inhibitors of the Hdm2:p53 interaction may offer advantages over these other approaches in terms of ease of delivery to the tumor site and uniform distribution; however, this also remains to be tested in the clinic.

We have focused on the discovery of small-molecule inhibitors of the Hdm2:p53 interaction and identified an active series of benzodiazepinediones (28, 32). Members of this chemical series have been successfully cocrystallized with Hdm2 and shown to make critical binding contacts in the p53-binding pocket of Hdm2 (28). Consistent with the submicromolar *in vitro* activity of the most potent of these compounds, the inhibitors selectively block cell growth of a variety of wt p53-expressing cells compared with mutant or null p53 tumor cell lines (Fig. 1; Table 1). These results imply that the activities observed *in vitro* are related to the growth inhibitory activities. Moreover, dissociation of the Hdm2:p53 complex in cells on short-term exposure to the benzodiazepinedione inhibitors provides further evidence that these compounds target the interface between Hdm2 and p53 in cells (Fig. 2A). Unlike DNA-damaging agents, such as doxorubicin, it was anticipated that direct disruption of Hdm2 from p53 would not induce phosphorylation of p53. Indeed, these compounds do not phosphorylate p53 at Ser^{15} nor H2AX and thus are not affecting p53 via some upstream-related activity (Fig. 2B and C). Overall, the correlation between the dose-dependent dissociation of Hdm2:p53 in cells and the inhibition of cellular growth elicited by these compounds supports the conclusion that inhibition of growth is due to antagonism of the Hdm2:p53 complex.

There are several lines of evidence that suggest that the Hdm2 oncoprotein can function independently of p53. Splice variants of Hdm2 lacking the p53-binding domain have been identified in human tumors and have been shown to possess transforming ability (55). *In vivo* studies have shown that the spectrum of tumors that develop in transgenic mice overexpressing Hdm2 is distinct from that found in p53-null mice and that Hdm2 can drive sarcomagenesis in p53-null animals (56). Lastly, other binding partners of Hdm2 could assist Hdm2 function along an oncogenic pathway [e.g., Hdm2 inhibition of MDM2-binding protein–induced p53-independent G_1 arrest (57)].

The benzodiazepinedione inhibitors described here lost potency in cells expressing Hdm2 in the absence of wt p53, supporting the conclusion that the compounds do not have direct effects on Hdm2 activities independent of p53 binding (Table 1). This was further addressed when we showed a similar response in Mdm2/p53 double-null mouse embryonic fibroblasts (29). Growth of these cells was inhibited by TDP521252 with an IC_{50} of 50 μmol/L (95% confidence limits, 38.2–65.3 μmol/L), which is ~3.5-fold less potent than with wt p53-expressing cells and similar to the average IC_{50} (46 μmol/L) observed in the mutant or null p53 cell lines (Table 1). Similar results were obtained with mouse embryonic fibroblasts rendered null to p53 and another Hdm2 family member known to regulate p53, MdmX (ref. 29; data not shown). Furthermore, in separate studies, we found that Hdm2-directed benzodiazepinediones did not bind to MdmX *in vitro* (data not shown). These results showed that the benzodiazepinediones did not induce Mdm2-dependent, p53-independent effects and did not interact with other Mdm2 family members.

We and others have observed that the earliest genes that are induced by p53 are involved in cell cycle arrest preceding genes associated with apoptosis (Fig. 3; ref. 58). It is of interest that this order of induction is observed, because it is known that cells can recover from cell cycle arrest (59). Perhaps this is a phenomenon associated with assessing the health of cells. The increase in expression of the apoptotic transcriptional targets of p53 coincides with the decrease in expression of the cell cycle control transcriptional targets. Whether sustained elevation of p53 is accomplished through naturally sensing DNA damage or artificially using approaches, such as small-molecule antagonists of the Hdm2:p53 interaction, the late induction of apoptotic genes may become functionally dominant depending on the cell type. In this regard, TDP521252 elicited an apoptotic response in HepG2 cells evidenced by caspase induction and the presence of condensed chromatin (Fig. 4), and we have observed similar responses in JAR choriocarcinoma cells. However, we and others (39) have also observed that sustained p53 levels alone do not dictate apoptosis for all cell

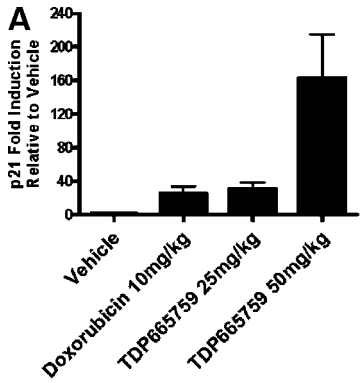

B

Agent	Response with TDP665759	Combination Index
5-Fluorouracil	Synergistic	0.59
Irinotecan	Synergistic	0.63
Doxorubicin	Synergistic	0.62
Cisplatin	Antagonistic	1.43

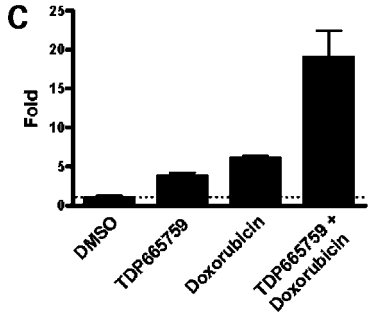

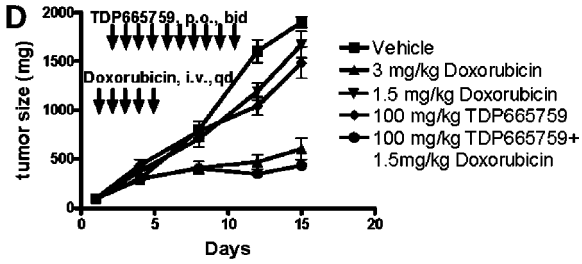

Figure 5. TDP665759 elicits p53 biomarker activity *in vivo* and synergizes with doxorubicin to suppress A375 tumor growth. **A,** TDP665759 induces p21 $^{waf1/cip1}$ *in vivo.* Nude mice were injected with 25 or 50 mg/kg TDP665759 i.p. b.i.d. for 4 d or 10 mg/kg doxorubicin once i.v. on day 3. Six hours after the first dose on day 4, mice were sacrificed and livers were harvested for total RNA extraction. Quantitative PCR was done to determine the relative ratios of p21 $^{waf1/cip1}$ in liver tissue. *Columns,* mean of three individual animals per group; *bars,* SD. **B,** drug combination effects in A375 melanoma cells. A375 melanoma cells were treated with TDP665759 and chemotherapeutic agents at the same time in a fixed ratio format. Cells were exposed to compound for 48 h before the determination of viable cells. Calculations of combination effects were done according to the method of Chou and Talalay (30) using CalcuSyn software. Combination indices of <0.9 are synergistic, between 0.9 and 1.1 are additive, and >1.1 are antagonistic and reported at the IC_{50}s for both agents. **C,** drug combinations synergistically induce total p53 levels. After adherence of A375 melanoma cells overnight, cells were treated with either 2 μmol/L TDP665759, 0.2 μmol/L doxorubicin, or the combination of 2 μmol/L TDP665759 and 0.2 μmol/L doxorubicin for 24 h. Cells were then lysed and total p53 levels were determined using the PathScan Total p53 Sandwich ELISA. *Columns,* average of duplicate treatments; *bars,* SD. **D,** TDP665759 enhances the activity of doxorubicin *in vivo*. A375 melanoma xenografts were established in female nude mice and allowed to reach 80 to 120 mg in size. At that time, mice were randomized into treatment groups, and treatment with vehicle (20.25% hydroxypropyl-β-cyclodextran, b.i.d. × 10), 100 mg/kg TDP665759 (b.i.d. × 10), 1.5 or 3 mg/kg doxorubicin (q.d. × 5), or a combination of 100 mg/kg TDP665759 (b.i.d. × 10) + 1.5 mg/kg doxorubicin (q.d. × 5) was initiated. Mice were monitored daily for general health and tumor size was measured every third or fourth day. Mice were euthanized when tumor volume exceeded 2 g. *Points,* mean tumor mass; *bars,* SD.

types. For example, caspase-3-null MCF7 cells (60) growth arrest but do not apoptose like HepG2 cells when treated with TDP521252 (data not shown), suggesting that p53 levels alone are not sufficient in all cell types to induce apoptosis and that this response will vary depending on the cellular environment.

One of the downstream consequences of activating p53 is the up-regulation of Hdm2 protein (Fig. 3B). The tight Hdm2 negative feedback loop induced by p53 activity has been well documented in the literature (13). Our analyses in cells showed that induction of Hdm2 expression is an early response to activation of p53 once it is dissociated from the complex by the inhibitors (Fig. 3A). Similarly, DNA-damaging chemotherapeutic agents, such as doxorubicin, also elicit an early induction of Hdm2, and in theory, this contributes to the long-term loss of efficacy of these drugs in man (61). One might anticipate that the combination of chemotherapeutic agents with an inhibitor of the Hdm2:p53 interaction would enhance the overall effect of blocking tumor growth. Indeed, such results have been shown with coadministration of antisense Hdm2 and 10-hydroxycamptothecin in SJSA xenografts (33). The benzodiazepinediones also act in synergy with a variety of chemotherapeutic agents in the A375 cell culture model (Fig. 5B) and this may be due to the higher levels of p53 in cells so treated (Fig. 5C). The mechanism by which cisplatin and inhibitors of the Hdm2:p53 interaction act antagonistically is uncertain at this time. However, these results are not unexpected, as cisplatin has been shown in multiple reports to be more efficacious when p53 is defective (62, 63).

The combination A375 xenograft study clearly shows that TDP665759 enhances the activity of doxorubicin *in vivo* (Fig. 5D). The combination of TDP665759 and doxorubicin at doses that are inactive alone led to a tumor growth delay (79% of control group) similar to doxorubicin at the maximum tolerated dose (74% of control group) at day 15 of the study. These results provide the first *in vivo* evidence that a small-molecule p53 agonist can potentiate DNA-damaging agents and thus may provide therapeutic benefit as a combination therapy.

Thus far, two other groups have reported small-molecule inhibitors of the hdm2:p53 interaction. Vassilev et al. identified *cis*-imidazoline derivatives (nutlins) that show cellular potencies similar to those reported here for the benzodiazepinediones (64). Although high doses of Nutlin-3 given twice daily were efficacious in preventing further tumor growth in a SJSA-1 xenograft study, it was not clearly established that the observed effects *in vivo* were mechanistically related to p53 antagonism. In contrast, RITA, another small-molecule inhibitor of the p53:Hdm2 interaction, was shown to decrease tumor growth in a HCT116 xenograft model and showed that efficacy coincides with stability of p53 in these tumors (65). However, RITA differs from the nutlins and from the benzodiazepinediones, because it has been reported to bind to p53; yet, this finding has recently been challenged (66). The compounds presented here produce molecular and cellular effects that are consistent with those induced by both the nutlins and RITA and additionally show that p53 agonists can enhance the *in vivo* efficacy of chemotherapeutic agents. Overall, our data support the concept that increasing p53 activity via disruption of the Hdm2:p53 interaction may have therapeutic use for the treatment of wt p53-expressing tumors.

Acknowledgments

We thank Piedmont Research Center for helpful discussions, Dr. Guillermina Lozano for the generous gift of mdm2/p53 double-null and mdmX/p53 double-null cell lines, Dr. Jan Sechler for helpful discussions and cells, Dr. Theodore Carver, Jennifer Lattanze, and Theresa McDevitt for technical assistance, Dr. Paul Wade and Sandra McKenney for assistance with microscopy, and Dr. Robert Tuman for assistance with statistical analyses.

References

1. Jones SN, Sands AT, Hancock AR, et al. The tumorigenic potential and cell growth characteristics of p53-deficient cells are equivalent in the presence or absence of Mdm2. Proc Natl Acad Sci U S A 1996;93:14106–11.

2. Keshelava N, Zuo JJ, Chen P, et al. Loss of p53 function confers high-level multidrug resistance in neuroblastoma cell lines. Cancer Res 2001;61:6185–93.

3. Johnston JB, Daeninck P, Verburg L, et al. p53, MDM-2, BAX and BCL-2 and drug resistance in chronic lymphocytic leukemia. Leuk Lymphoma 1997;26:435–49.

4. Buttitta F, Marchetti A, Gadducci A, et al. p53 alterations are predictive of chemoresistance and aggressiveness in ovarian carcinomas: a molecular and immunohistochemical study. Br J Cancer 1997;75:230–5.

5. Zhou BP, Liao Y, Xia W, Zou Y, Spohn B, Hung MC. HER-2/*neu* induces p53 ubiquitination via Akt-mediated MDM2 phosphorylation. Nat Cell Biol 2001;3:973–82.

6. Coukos G, Rubin SC. Chemotherapy resistance in ovarian cancer: new molecular perspectives. Obstet Gynecol 1998;91:783–92.

7. Harada T, Ogura S, Yamazaki K, et al. Predictive value of expression of p53, Bcl-2 and lung resistance-related protein for response to chemotherapy in non-small cell lung cancers. Cancer Sci 2003;94:394–9.

8. Yamazaki Y, Chiba I, Hirai A, et al. Radioresistance in oral squamous cell carcinoma with p53 DNA contact mutation. Am J Clin Oncol 2003;26:e124–9.

9. Beroud C, Soussi T. p53 gene mutation: software and database. Nucleic Acids Res 1998;26:200–4.

10. Momand J, Jung D, Wilczynski S, Niland J. The MDM2 gene amplification database. Nucleic Acids Res 1998;26:3453–9.

11. Chene P. Targeting p53 in cancer. Curr Med Chem Anti-Canc Agents 2001;1:151–61.

12. Chene P. Inhibiting the p53-MDM2 interaction: an important target for cancer therapy. Nat Rev Cancer 2003;3:102–9.

13. Wu X, Bayle JH, Olson D, Levine AJ. The p53-mdm-2 autoregulatory feedback loop. Genes Dev 1993;7:1126–32.

14. Jones SN, Roe AE, Donehower LA, Bradley A. Rescue of embryonic lethality in Mdm2-deficient mice by absence of p53. Nature 1995;378:206–8.

15. Montes de Oca Luna R, Wagner DS, Lozano G. Rescue of early embryonic lethality in mdm2-deficient mice by deletion of p53. Nature 1995;378:203–6.

16. Bottger A, Bottger V, Garcia-Echeverria C, et al. Molecular characterization of the hdm2-p53 interaction. J Mol Biol 1997;269:744–56.

17. Honda R, Tanaka H, Yasuda H. Oncoprotein MDM2 is a ubiquitin ligase E3 for tumor suppressor p53. FEBS Lett 1997;420:25–7.

18. Suzuki A, Toi M, Yamamoto Y, Saji S, Muta M, Tominaga T. Role of MDM2 overexpression in doxorubicin resistance of breast carcinoma. Jpn J Cancer Res 1998;89:221–7.

19. Zhou M, Gu L, Abshire TC, et al. Incidence and prognostic significance of MDM2 oncoprotein overexpression in relapsed childhood acute lymphoblastic leukemia. Leukemia 2000;14:61–7.

20. Ikeguchi M, Ueda T, Fukuda K, Yamaguchi K, Tsujitani S, Kaibara N.

Expression of the murine double minute gene 2 oncoprotein in esophageal squamous cell carcinoma as a novel marker for lack of response to chemoradiotreatment. Am J Clin Oncol 2002;25:454 – 9.

21. Chen L, Agrawal S, Zhou W, Zhang R, Chen J. Synergistic activation of p53 by inhibition of MDM2 expression and DNA damage. Proc Natl Acad Sci U S A 1998;95:195 – 200.

22. Chen L, Lu W, Agrawal S, Zhou W, Zhang R, Chen J. Ubiquitous induction of p53 in tumor cells by antisense inhibition of MDM2 expression. Mol Med 1999;5:21 – 34.

23. Tortora G, Caputo R, Damiano V, et al. A novel MDM2 anti-sense oligonucleotide has anti-tumor activity and potentiates cytotoxic drugs acting by different mechanisms in human colon cancer. Int J Cancer 2000;88:804 – 9.

24. Bottger A, Bottger V, Sparks A, Liu WL, Howard SF, Lane DP. Design of a synthetic Mdm2-binding mini protein that activates the p53 response *in vivo*. Curr Biol 1997;7:860 – 9.

25. Wang H, Nan L, Yu D, Agrawal S, Zhang R. Antisense anti-MDM2 oligonucleotides as a novel therapeutic approach to human breast cancer: *in vitro* and *in vivo* activities and mechanisms. Clin Cancer Res 2001;7:3613 – 24.

26. Pearson S, Jia H, Kandachi K. China approves first gene therapy. Nat Biotechnol 2004;22:3 – 4.

27. Lane DP, Lain S. Therapeutic exploitation of the p53 pathway. Trends Mol Med 2002;8:S38 – 42.

28. Grasberger BL, Lu T, Schubert C, et al. Discovery and cocrystal structure of benzodiazepinedione Hdm2 antagonists that activate p53 in cells. J Med Chem 2005;48:909 – 12.

29. Parant J, Chavez-Reyes A, Little NA, et al. Rescue of embryonic lethality in Mdm4-null mice by loss of Trp53 suggests a nonoverlapping pathway with MDM2 to regulate p53. Nat Genet 2001;29: 92 – 5.

30. Chou TC, Talalay P. Quantitative analysis of dose-effect relationships: the combined effects of multiple drugs or enzyme inhibitors. Adv Enzyme Regul 1984;22:27 – 55.

31. Pantoliano MW, Petrella EC, Kwasnoski JD, et al. High-density miniaturized thermal shift assays as a general strategy for drug discovery. J Biomol Screen 2001;6:429 – 40.

32. Parks DJ, Lafrance LV, Calvo RR, et al. 1,4-Benzodiazepine-2,5-diones as small molecule antagonists of the HDM2-p53 interaction: discovery and SAR. Bioorg Med Chem Lett 2005;15:765 – 70.

33. Wang H, Zeng X, Oliver P, et al. MDM2 oncogene as a target for cancer therapy: an antisense approach. Int J Oncol 1999;15:653 – 60.

34. Milczarek GJ, Martinez J, Bowden GT. p53 Phosphorylation: biochemical and functional consequences. Life Sci 1997;60:1 – 11.

35. Meek DW. Post-translational modification of p53. Semin Cancer Biol 1994;5:203 – 10.

36. Thompson T, Tovar C, Yang H, et al. Phosphorylation of p53 on key serines is dispensable for transcriptional activation and apoptosis. J Biol Chem 2004;279:53015 – 22.

37. Lee TK, Lau TC, Ng IO. Doxorubicin-induced apoptosis and chemosensitivity in hepatoma cell lines. Cancer Chemother Pharmacol 2002; 49:78 – 86.

38. Levine AJ. p53, the cellular gatekeeper for growth and division. Cell 1997;88:323 – 31.

39. Slee EA, O'Connor DJ, Lu X. To die or not to die: how does p53 decide? Oncogene 2004;23:2809 – 18.

40. Flatt PM, Polyak K, Tang LJ, et al. p53-dependent expression of PIG3 during proliferation, genotoxic stress, and reversible growth arrest. Cancer Lett 2000;156:63 – 72.

41. Kaeser MD, Iggo RD. Chromatin immunoprecipitation analysis fails to support the latency model for regulation of p53 DNA binding activity *in vivo*. Proc Natl Acad Sci U S A 2002;99:95 – 100.

42. Yeh PY, Chuang SE, Yeh KH, Song YC, Chang LL, Cheng AL. Phosphorylation of p53 on Thr^{55} by ERK2 is necessary for doxorubicin-induced p53 activation and cell death. Oncogene 2004;23:3580 – 8.

43. Fei P, Bernhard EJ, El-Deiry WS. Tissue-specific induction of p53 targets *in vivo*. Cancer Res 2002;62:7316 – 27.

44. Bartel F, Harris LC, Wurl P, Taubert H. MDM2 and its splice variant messenger RNAs: expression in tumors and down-regulation using antisense oligonucleotides. Mol Cancer Res 2004;2:29 – 35.

45. Kawabe S, Munshi A, Zumstein LA, Wilson DR, Roth JA, Meyn RE. Adenovirus-mediated wild-type p53 gene expression radiosensitizes non-small cell lung cancer cells but not normal lung fibroblasts. Int J Radiat Biol 2001;77:185 – 94.

46. Prasad G, Wang H, Agrawal S, Zhang R. Antisense anti-MDM2 oligonucleotides as a novel approach to the treatment of glioblastoma multiforme. Anticancer Res 2002;22:107 – 16.

47. Wang H, Yu D, Agrawal S, Zhang R. Experimental therapy of human prostate cancer by inhibiting MDM2 expression with novel mixed-backbone antisense oligonucleotides: *in vitro* and *in vivo* activities and mechanisms. Prostate 2003;54:194 – 205.

48. Zhang Z, Wang H, Prasad G, et al. Radiosensitization by antisense anti-MDM2 mixed-backbone oligonucleotide in *in vitro* and *in vivo* human cancer models. Clin Cancer Res 2004;10:1263 – 73.

49. Cristofanilli M, Khrisnamurthy S, Guerra L, et al. Advexin® (Ad5CMV-p53) combined with docetaxel (T) and doxorubicin (D) as induction chemotherapy (IC): efficacy of a novel gene-therapy approach for patients with locally advanced breast cancer (LABC). 27th Annual San Antonio Breast Cancer Symposium; San Antonio TX; 2004.

50. Haapajarvi T, Pitkanen K, Laiho M. Human melanoma cell line UV responses show independency of p53 function. Cell Growth Differ 1999; 10:163 – 71.

51. Donehower LA, Harvey M, Slagle BL, et al. Mice deficient for p53 are developmentally normal but susceptible to spontaneous tumours. Nature 1992;356:215 – 21.

52. Hollstein M, Hergenhahn M, Yang Q, Bartsch H, Wang ZQ, Hainaut P. New approaches to understanding p53 gene tumor mutation spectra. Mutat Res 1999;431:199 – 209.

53. Hainaut P. Tumor-specific mutations in p53: the acid test. Nat Med 2002;8:21 – 3.

54. Zeimet A, Marth C. Why did p53 gene therapy fail in ovarian cancer? Lancet Oncol 2003;4:415 – 22.

55. Sigalas I, Calvert AH, Anderson JJ, Neal DE, Lunec J. Alternatively spliced mdm2 transcripts with loss of p53 binding domain sequences: transforming ability and frequent detection in human cancer. Nat Med 1996;2:912 – 7.

56. Jones SN, Hancock AR, Vogel H, Donehower LA, Bradley A. Overexpression of Mdm2 in mice reveals a p53-independent role for Mdm2 in tumorigenesis. Proc Natl Acad Sci U S A 1998;95: 15608 – 12.

57. Boyd MT, Vlatkovic N, Haines DS. A novel cellular protein (MTBP) binds to MDM2 and induces a G_1 arrest that is suppressed by MDM2. J Biol Chem 2000;275:31883 – 90.

58. Reinke V, Lozano G. The p53 targets mdm2 and Fas are not required as mediators of apoptosis *in vivo*. Oncogene 1997;15:1527 – 34.

59. Ha L, Ceryak S, Patierno SR. Chromium (VI) activates ataxia telangiectasia mutated (ATM) protein. Requirement of ATM for both apoptosis and recovery from terminal growth arrest. J Biol Chem 2003; 278:17885 – 94.

60. Wolf BB, Schuler M, Echeverri F, Green DR. Caspase-3 is the primary activator of apoptotic DNA fragmentation via DNA fragmentation factor-45/inhibitor of caspase-activated DNase inactivation. J Biol Chem 1999;274:30651 – 6.

61. Isaacs JS, Saito S, Neckers LM. Requirement for HDM2 activity in the rapid degradation of p53 in neuroblastoma. J Biol Chem 2001;276: 18497 – 506.

62. Fan S, Smith ML, Rivet DJ, II, et al. Disruption of p53 function sensitizes breast cancer MCF-7 cells to cisplatin and pentoxifylline. Cancer Res 1995;55:1649 – 54.

63. Bauer JA, Trask DK, Kumar B, et al. Reversal of cisplatin resistance with a BH3 mimetic, (−)-gossypol, in head and neck cancer cells: role of wild-type p53 and Bcl-x_L. Mol Cancer Ther 2005;4:1096 – 104.

64. Vassilev LT, Vu BT, Graves B, et al. *In vivo* activation of the p53 pathway by small-molecule antagonists of MDM2. Science 2004;303: 844 – 8.

65. Issaeva N, Bozko P, Enge M, et al. Small molecule RITA binds to p53, blocks p53-HDM-2 interaction and activates p53 function in tumors. Nat Med 2004;10:1321 – 8.

66. Krajewski M, Ozdowy P, D'Silva L, Rothweiler U, Holak TA. NMR indicates that the small molecule RITA does not block p53-MDM2 binding *in vitro*. Nat Med 2005;11:1135 – 6.

Molecular Cancer Therapeutics

Benzodiazepinedione inhibitors of the Hdm2:p53 complex suppress human tumor cell proliferation *in vitro* and sensitize tumors to doxorubicin *in vivo*

Holly K. Koblish, Shuyuan Zhao, Carol F. Franks, et al.

Mol Cancer Ther 2006;5:160-169.